Polymer Journal (2012) 44, 42–50

www.nature.com/pj

ORIGINAL ARTICLE

Amplification of macromolecular helicity of dynamic helical poly(phenylacetylene)s bearing non-racemic alanine pendants in dilute solution, liquid crystal and two-dimensional crystal

Sousuke Ohsawa[1,2], Shin-ichiro Sakurai[2], Kanji Nagai[1,2,3], Katsuhiro Maeda[1,4], Jiro Kumaki[2,5] and Eiji Yashima[1,2]

Optically active poly(phenylacetylene) copolymers composed of non-racemic phenylacetylenes bearing L- and D-alanine decyl esters as the side groups (poly($1L_m$-*co*-$1D_n$), m > n) were prepared by the copolymerization of the corresponding L- and D-phenylacetylenes with different enantiomeric excesses using a rhodium catalyst; their chiral amplification of the helical conformation as an excess of one-handedness in a dilute solution, in a lyotropic liquid-crystalline (LC) state and in a two-dimensional (2D) crystal on substrate was investigated by measuring the circular dichroism spectra of the copolymers at different temperatures, mesoscopic cholesteric twist in the LC state (cholesteric helical pitch) and high-resolution atomic force microscopy images of the self-assembled 2D helix-bundle structures of the copolymer chains, respectively.
Polymer Journal (2012) **44,** 42–50; doi:10.1038/pj.2011.37; published online 18 May 2011

Keywords: atomic force microscopy; chiral amplification; chirality; circular dichroism; helical structure; helix inversion; liquid crystal

INTRODUCTION

Chiral amplification is a unique and attractive process from which a small chiral bias is highly enhanced through covalent or non-covalent bonding interactions.[1–6] Starting with the pioneering work carried out by Green *et al.*[1,7,8] in polymeric systems using stiff, rod-like polyisocyanates, the substantial feature of the dynamic macromolecular helicity of polyisocyanates, which consist of right- and left-handed helical segments separated by energetically unfavorable, rarely occurring helical reversals, has been experimentally and theoretically revealed. Green *et al.* demonstrated that copolymerization of achiral isocyanates with a tiny amount of optically active ones, or copolymerization of non-racemic isocyanates with a small enantiomeric excess (ee), produced optically active polyisocyanates with a greater excess of one-handed helical conformation, and termed these highly cooperative processes as the 'sergeants and soldiers effect'[7] and 'majority rule',[8] respectively. These unique chiral amplification phenomena have been now observed in other varieties of covalent and non-covalent polymeric[6,9–14] and supramolecular helical systems[3–6] involving non-covalent helical assemblies consisting of chiral–achiral or chiral–chiral (*R*/*S*) small molecular components.

Green *et al.*[15] further extended the principle to the liquid crystalline (LC) systems, and found that the helical-sense bias of optically active polyisocyanates was further amplified in the polymer backbones as a greater excess of a single-handed helix through self-assembly into a lyotropic cholesteric liquid crystal; this effect was considered to be due to the reduction in population of the energetically unfavorable, kinked helical reversals in the LC state. A similar, but non-covalent, hierarchical amplification of helical chirality was observed for a dynamic helical, charged poly(phenylacetylene) in water.[16–18]

Recently, we have reported a unique amplification of macromolecular helicity of dynamic helical poly(phenylacetylene)s copolymers composed of optically active and achiral phenylacetylenes bearing L-alanine decyl esters (**1L**) and 2–aminoisobutylic acid decyl esters (**Aib**) as the pendant groups, respectively, (poly($\mathbf{1L}_m$-*co*-$\mathbf{Aib}_n$)), in the cholesteric LC state and two-dimensional (2D) crystals on substrate.[19] Mesoscopic cholesteric twist (cholesteric helical pitch) in the LC state of the copolymers in concentrated solutions and high-resolution atomic force microscopy (AFM) images of the self-assembled 2D helix bundles of the copolymer chains on substrate enabled us to determine the helical-sense excesses of the copolymers, leading to a

[1]Department of Molecular Design and Engineering, Graduate School of Engineering, Nagoya University, Nagoya, Japan and [2]Yashima Super-structured Helix Project, Exploratory Research for Advanced Technology (ERATO), Japan Science and Technology Agency (JST), Nagoya, Japan
Correspondence: Professor E Yashima, Department of Molecular Design and Engineering, Graduate School of Engineering, Nagoya University, Chikusa-ku, Nagoya 464-8603, Japan.
E-mail: yashima@apchem.nagoya-u.ac.jp
[3]Current address: Department of Applied Chemistry, Graduate School of Engineering, Nagoya University.
[4]Current address: Graduate School of Natural Science and Technology, Kanazawa University, Kakuma-machi, Kanazawa 920-1192, Japan.
[5]Current address: Department of Polymer Science and Engineering, Graduate School of Science and Engineering, Yamagata University, 4-3-16, Jonan, Yonezawa, Yamagata 992-8510, Japan.
Received 21 January 2011; revised 21 March 2011; accepted 25 March 2011; published online 18 May 2011

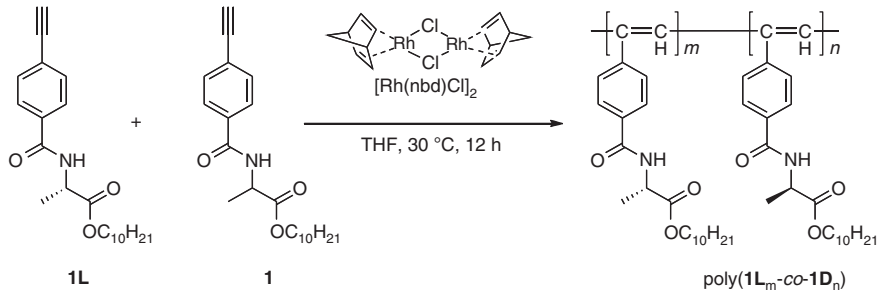

Scheme 1 Synthesis of poly($\mathbf{1L}_m$-*co*-$\mathbf{1D}_n$).

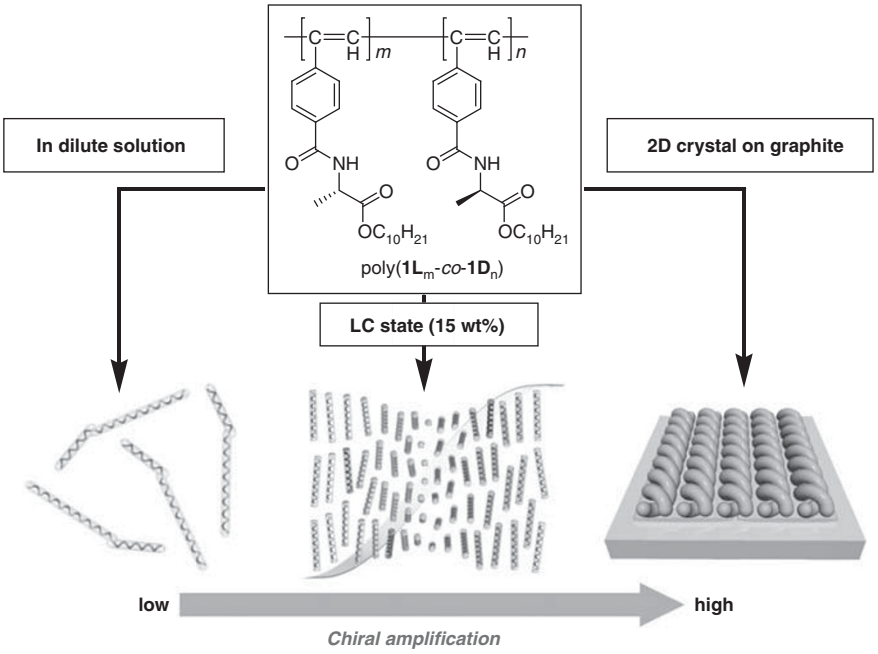

Figure 1 Schematic illustration of chiral amplification in macromolecular helicity of poly($\mathbf{1L}_m$-*co*-$\mathbf{1D}_n$) in dilute solution (left), in liquid-crystalline (LC) state (middle) and in the two-dimensional (2D) crystal formed on graphite (right). Excess of one-handed helical sense (right- or left-handed helix) of poly($\mathbf{1L}_m$-*co*-$\mathbf{1D}_n$) in dilute solution is amplified in the LC state and in the 2D crystal, resulting in a cholesteric LC phase and 2D helix bundle, respectively. A full color version of this figure is available at *Polymer Journal* online.

conclusion that the macromolecular helicity of poly($\mathbf{1L}_m$-*co*-$\mathbf{Aib}_n$)s was hierarchically amplified in the order of the dilute solution, in LC state and 2D crystal (sergeants and soldiers effect).

In this study, we report the synthesis of a series of dynamic helical poly(phenylacetylene) copolymers consisting of non-racemic phenylacetylenes bearing L- and D-alanine decyl esters as the pendant groups with different ee values (poly($\mathbf{1L}_m$-*co*-$\mathbf{1D}_n$), m > n) (Scheme 1); their chiral amplification in macromolecular helicity ('majority rule' effect) in a dilute solution, in a lyotropic LC state and in a 2D crystal on substrate was investigated by measuring the circular dichroism (CD) spectra of the copolymers, mesoscopic cholesteric twist in the LC state and high-resolution AFM images of the self-assembled 2D helix bundle structures of the copolymer chains, respectively. We anticipated that the macromolecular helicity with an excess single-handed helix induced in poly($\mathbf{1L}_m$-*co*-$\mathbf{1D}_n$) in a dilute solution could be further amplified in the copolymer backbones as a greater excess of a single-handed helix through self-assemblies into the lyotropic cholesteric LC state as well as in the 2D crystals on substrate; the latter will be directly visualized by high-resolution AFM (Figure 1).

EXPERIMENTAL PROCEDURE

Instruments

NMR spectra were taken on a Varian VXR-500S spectrometer (Palo Alto, CA, USA) operating at 500 MHz for ^{1}H and 125 MHz for ^{13}C, respectively, using tetramethylsilane as the internal standard. IR spectra were recorded on a JASCO Fourier Transform IR-620 spectrometer (Hachioji, Japan). The absorption and CD spectra were measured in a 1.0-mm quartz cell on a JASCO V570 spectrophotometer and a JASCO J-725 spectropolarimeter, respectively. Temperature was controlled with JASCO ETC-505T and PTC-423L instruments for absorption and CD measurements, respectively. The polymer concentration was calculated on the basis of the monomer units and was found to be 0.3 mg ml^{-1}. Laser Raman spectra were recorded on a JASCO RMP200 spectrometer. Polarizing optical microscopic observations were carried out with an OPTIPHOTO-POL polarizing optical microscope (Nikon, Tokyo, Japan) equipped with a DS-5M CCD camera (Nikon) connected to a DS-L1 control unit (Nikon). The sample solution was sealed in a glass capillary tube to observe the fingerprint texture at ambient temperature (20–25 °C). Size-exclusion chromatography measurements were recorded with a JASCO PU-980 liquid chromatograph equipped with a UV–visible detector (254 nm, JASCO UV-970) and a column oven (JASCO CO-965). A size-exclusion

chromatography column (Tosoh TSK-GEL Multipore H_{XL}-M column, Tokyo, Japan) was connected, and chloroform was used as the eluent at a flow rate of 1.0 ml min^{-1} at 40 °C. The molecular-weight calibration curve was obtained with standard polystyrenes (Tosoh). Optical rotation was measured on a JASCO P-1030 polarimeter in a 2-cm quartz cell at 25 °C equipped with a temperature controller (EYELA NCB-2100, Tokyo, Japan).

Materials

THF was dried over sodium benzophenone ketyl, distilled onto lithium aluminium hydride under nitrogen and distilled under high vacuum just before use. Benzene (water content <30 p.p.m.) and $[Rh(nbd)Cl]_2$ (nbd=norbornadiene) were obtained from Aldrich (Milwaukee, WI, USA). Triethylamine was purchased from Wako (Osaka, Japan), then distilled and dried over KOH pellets under nitrogen. Monomer **1L** and racemic monomer **1** were prepared according to a previously reported method.[19,20] Poly($\mathbf{1L}_m$-*co*-$\mathbf{1D}_n$)s were synthesized according to Scheme 1 by the copolymerization of **1L** and **1** with $[Rh(nbd)Cl]_2$ in THF.

Polymerization

Polymerization was carried out in a dry glass ampule under a dry nitrogen atmosphere with $[Rh(nbd)Cl]_2$ as the catalyst. A typical polymerization procedure is described below.

Monomer **1L** (0.10 g, 0.28 mmol) and racemic monomer **1** (0.10 g, 0.28 mmol) were placed into a dry ampule. After the mixture was dried *in vacuo* at room temperature for 3 h, dry THF (1.0 ml) and triethylamine (0.075 ml) were added with a syringe. A part of the mixture was withdrawn before the polymerization and the precise ee of the mixture was estimated to be 50% ee by HPLC using a Chiralpak AD-H column (25×0.46 (i.d.) cm; Daicel, Osaka, Japan), with hexane-2-propanol (9/1, v/v) as the eluent. A solution of $[Rh(nbd)Cl]_2$ in THF was then added at room temperature. The concentrations of the monomer and the rhodium catalyst were 0.5 and 0.0025 M, respectively. The polymerization rapidly proceeded and an orange-colored polymer gel appeared within a few seconds. After 12 h at 30 °C, the resulting copolymer was precipitated into a large amount of methanol, collected by centrifugation and dried *in vacuo* at room temperature overnight. The obtained copolymer was dissolved in a small amount of benzene and lyophilized (90% yield). The stereoregularity of the copolymer was investigated by laser Raman spectroscopy and was highly *cis-transoidal* because its ^{1}H NMR spectrum was too broad to determine the stereoregularity (Supplementary Figure S1). In the same way, the copolymerizations of **1L** and **1** with different ee values were performed and the copolymerization results are summarized in Table 1.

Table 1 Copolymerization results of 1L and racemic 1 with $[Rh(nbd)Cl]_2$ in THF at 30 °C for 12 h[a]

	%ee of **1**	Copolymer			
Run	(L rich)[b]	Sample code	Yield (%)[c]	$M_n\times10^{-4}$[d]	M_w/M_n[d]
1	1.3	poly($\mathbf{1L}_{0.505}$-*co*-$\mathbf{1D}_{0.495}$)	93	18.1	4.6
2	5.4	poly($\mathbf{1L}_{0.525}$-*co*-$\mathbf{1D}_{0.475}$)	90	10.4	9.4
3	10	poly($\mathbf{1L}_{0.55}$-*co*-$\mathbf{1D}_{0.45}$)	92	15.7	5.6
4	30	poly($\mathbf{1L}_{0.65}$-*co*-$\mathbf{1D}_{0.35}$)	91	14.5	5.4
5	50	poly($\mathbf{1L}_{0.75}$-*co*-$\mathbf{1D}_{0.25}$)	90	18.0	5.1
6	70	poly($\mathbf{1L}_{0.85}$-*co*-$\mathbf{1D}_{0.15}$)	91	14.3	9.1
7	90	poly($\mathbf{1L}_{0.95}$-*co*-$\mathbf{1D}_{0.05}$)	93	22.3	4.4
8	100	poly-**1L**	94	31.4	4.9

Abbreviations: ee, enantiomeric excess; nbd, norbornadiene; THF, tetrahydrofuran; M_n, number-average molecular weight; M_w, weight-average molecular weight.
[a][Monomers] = 0.5 M, [[Rh(nbd)Cl]$_2$]=0.0025 M.
[b]Estimated by chiral HPLC using a Chiralpak AD-H column.
[c]Methanol–insoluble fraction. The molar ratios of **1L** and **1D** in the copolymers were presumed to be equal to the feed molar ratios because the copolymerizations almost quantitatively afforded the copolymers.
[d]Determined by size-exclusion chromatography in chloroform using polystyrene standards.

Spectroscopic data of poly($\mathbf{1L}_{0.505}$-*co*-$\mathbf{1D}_{0.495}$) (1.3% ee, run 1 in Table 1): IR (benzene solution, cm^{-1}): 3275 (ν_{NH}), 1750 ($\nu_{C=O}$ ester), 1636 (amide I), 1540 (amide II). ^{1}H NMR ($CDCl_3$, 55 °C, 500 MHz): δ 0.87 (t, CH_3, 3H), 1.26 (s, CH_2, 14H), 1.44 (br, CH_3, 3H), 1.59 (br, CH_2, 2H), 4.12 (br, CH_2, 2H), 4.62 (br, CH, 1H), 5.82 (br, =CH, 1H), 6.57 (br, aromatic, 2H), 7.26 (br, aromatic, 2H). Anal. calcd. (%) for $(C_{23}H_{33}NO_3)_n$: C, 73.91; H, 8.74; N, 3.92. Found: C, 73.76; H, 8.80; N, 3.93. $[\alpha]_D^{25}$ –4.5° (*c* 0.1, benzene).

Spectroscopic data of poly($\mathbf{1L}_{0.525}$-*co*-$\mathbf{1D}_{0.475}$) (5.4% ee, run 2 in Table 1): IR (benzene solution, cm^{-1}): 3277 (ν_{NH}), 1750 ($\nu_{C=O}$ ester), 1636 (amide I), 1540 (amide II). ^{1}H NMR ($CDCl_3$, 55 °C, 500 MHz): δ 0.86 (t, CH_3, 3H), 1.25 (s, CH_2, 14H), 1.59 (br, CH_3, 3H), 1.59 (br, CH_2, 2H), 4.09 (br, CH_2, 2H), 4.62 (br, CH, 1H), 5.81 (br, =CH, 1H), 6.56 (br, aromatic, 2H), 7.46 (br, aromatic, 2H). Anal. calcd. (%) for $(C_{23}H_{33}NO_3)_n$: C, 73.91; H, 8.74; N, 3.92. Found: C, 73.75; H, 8.75; N, 3.84. $[\alpha]_D^{25}$ –35.0° (*c* 0.1, benzene).

Spectroscopic data of poly($\mathbf{1L}_{0.55}$-*co*-$\mathbf{1D}_{0.45}$) (10% ee, run 3 in Table 1): IR (benzene solution, cm^{-1}): 3277 (ν_{NH}), 1750 ($\nu_{C=O}$ ester), 1636 (amide I), 1540 (amide II). ^{1}H NMR ($CDCl_3$, 55 °C, 500 MHz): δ 0.88 (t, CH_3, 3H), 1.25 (s, CH_2, 14H), 1.55 (br, CH_3, CH_2 5H), 4.09 (br, CH_2, 2H), 4.62 (br, CH, 1H), 5.82 (br, =CH, 1H), 6.53 (br, aromatic, 2H), 7.33 (br, aromatic, 2H). Anal. calcd. (%) for $(C_{23}H_{33}NO_3)_n$: C, 73.91; H, 8.74; N, 3.92. Found: C, 74.05; H, 8.87; N, 3.84. $[\alpha]_D^{25}$ –59.0° (*c* 0.1, benzene).

Spectroscopic data of poly($\mathbf{1L}_{0.65}$-*co*-$\mathbf{1D}_{0.35}$) (30% ee, run 4 in Table 1): IR (benzene solution, cm^{-1}): 3278 (ν_{NH}), 1750 ($\nu_{C=O}$ ester), 1635 (amide I), 1540 (amide II). ^{1}H NMR ($CDCl_3$, 55 °C, 500 MHz): δ 0.86 (t, CH_3, 3H), 1.25 (s, CH_2, 14H), 1.41 (br, CH_3, 3H), 1.52 (br, CH_2, 2H), 4.06 (br, CH_2, 2H), 4.55 (br, CH, 1H), 5.74 (br, =CH, 1H), 6.48 (br, aromatic, 2H), 7.27 (br, aromatic, 2H). Anal. calcd. (%) for $(C_{23}H_{33}NO_3)_n$: C, 73.91; H, 8.74; N, 3.92. Found: C, 73.93; H, 8.93; N, 3.81. $[\alpha]_D^{25}$ –58.5° (*c* 0.1, benzene).

Spectroscopic data of poly($\mathbf{1L}_{0.75}$-*co*-$\mathbf{1D}_{0.25}$) (50% ee, run 5 in Table 1): IR (benzene solution, cm^{-1}): 3278 (ν_{NH}), 1749 ($\nu_{C=O}$ ester), 1635 (amide I), 1540 (amide II). ^{1}H NMR ($CDCl_3$, 55 °C, 500 MHz): δ 0.86 (t, CH_3, 3H), 1.25 (s, CH_2, 14H), 1.43 (br, CH_3, 3H), 1.58 (br, CH_2, 2H), 4.08 (br, CH_2, 2H), 4.62 (br, CH, 1H), 5.81 (br, =CH, 1H), 6.55 (br, aromatic, 2H), 7.25 (br, aromatic, 2H). Anal. Calcd. (%) for $(C_{23}H_{33}NO_3)_n$: C, 73.91; H, 8.74; N, 3.92. Found: C, 73.73; H, 8.79; N, 4.08. $[\alpha]_D^{25}$ –54.0° (*c* 0.1, benzene).

Spectroscopic data of poly($\mathbf{1L}_{0.85}$-*co*-$\mathbf{1D}_{0.15}$) (70% ee, run 6 in Table 1): IR (benzene solution, cm^{-1}): 3277 (ν_{NH}), 1751 ($\nu_{C=O}$ ester), 1635 (amide I), 1540 (amide II). ^{1}H NMR ($CDCl_3$, 55 °C, 500 MHz): δ 0.86 (t, CH_3, 3H), 1.25 (s, CH_2, 14H), 1.57 (br, CH_3, 3H), 1.41 (br, CH_2, 2H), 4.05 (br, CH_2, 2H), 4.63 (br, CH, 1H), 5.84 (br, =CH, 1H), 6.53 (br, aromatic, 2H), 7.46 (br, aromatic, 2H). Anal. calcd. (%) for $(C_{23}H_{33}NO_3)_n$: C, 73.91; H, 8.74; N, 3.92. Found: C, 73.86; H, 8.76; N, 3.78. $[\alpha]_D^{25}$ –53.5° (*c* 0.1, benzene).

Spectroscopic data of poly($\mathbf{1L}_{0.95}$-*co*-$\mathbf{1D}_{0.05}$) (90% ee, run 7 in Table 1): IR (benzene solution, cm^{-1}): 3277 (ν_{NH}), 1751 ($\nu_{C=O}$ ester), 1635 (amide I), 1540 (amide II). ^{1}H NMR ($CDCl_3$, 55 °C, 500 MHz): δ 0.86 (t, CH_3, 3H), 1.25 (s, CH_2, 14H), 1.41 (br, CH_3, 3H), 1.56 (br, CH_2, 2H), 4.07 (br, CH_2, 2H), 4.66 (br, CH, 1H), 5.87 (br, =CH, 1H), 6.47 (br, aromatic, 2H), 7.46 (br, aromatic, 2H). Anal. calcd. (%) for $(C_{23}H_{33}NO_3)_n$: C, 73.91; H, 8.74; N, 3.92. Found: C, 73.76; H, 8.95; N, 3.84. $[\alpha]_D^{25}$ –50.5° (*c* 0.1, benzene).

Spectroscopic data of poly-**1L** (100% ee, run 8 in Table 1): IR (benzene solution, cm^{-1}): 3277 (ν_{NH}), 1751 ($\nu_{C=O}$ ester), 1635 (amide I), 1540 (amide II). ^{1}H NMR ($CDCl_3$, 55 °C, 500 MHz): δ 0.86 (t, CH_3, 3H), 1.25 (s, CH_2, 14H), 1.41 (br, CH_3, 3H), 1.59 (br, CH_2, 2H), 4.04 (br, CH_2, 2H), 4.66 (br, CH, 1H), 5.90 (br, =CH, 1H), 6.51 (br, aromatic, 2H), 7.46 (br, aromatic, 2H). Anal. Calcd. (%) for $(C_{23}H_{33}NO_3)_n$: C, 73.91; H, 8.74; N, 3.92. Found: C, 74.09; H, 8.88; N, 3.89. $[\alpha]_D^{25}$ –51.0° (*c* 0.1, benzene).

AFM Measurements

The AFM measurements were recorded according to a previously reported procedure.[21–23] A typical experimental procedure is described below. Stock solutions of poly($\mathbf{1L}_m$-*co*-$\mathbf{1D}_n$) in dry benzene (0.005 mg ml^{-1}) were prepared. Samples for the AFM measurements of the copolymers were prepared by casting 40-μl aliquots of the stock solutions on freshly cleaved HOPG substrate at room temperature (25 °C), and the solvents were then evaporated slowly under a benzene vapor atmosphere. After the copolymers had been deposited on the HOPG, the substrates of HOPG were exposed to a benzene vapor for

12 h, and the substrates were then dried under vacuum for 2 h. The AFM measurements were recorded using a Nanoscope IIIa microscope (Veeco Instruments, Santa Barbara, CA, USA) in air at ambient temperature, with standard silicon cantilevers (NCH, NanoWorld, Neuchâtel, Switzerland) in the tapping mode. The typical settings of the AFM for the high-magnification observations were as follows: the free amplitude of the oscillation frequency of ~1.0–1.5 V, the set-point amplitude of 0.9–1.4 V and a scan rate of 2.5 Hz. The Nanoscope image processing software was used for the image analysis.

RESULTS AND DISCUSSION

The optically active poly(phenylacetylene) copolymers (poly(**1L**$_m$-*co*-**1D**$_n$) m > n) bearing L- and D-alanine decyl esters as the pendant groups with different ee values were synthesized by the copolymerization of the enantiomerically pure **1L** and racemic monomer **1** with a rhodium complex $[Rh(nbd)Cl]_2$ in tetrahydrofuran (THF), according to a method previously reported (Scheme 1).[19,20] All copolymers soluble in most common organic solvents, such as benzene, toluene, THF, chloroform and carbon tetrachloride (CCl_4), with relatively high molecular weights (M_n=1.0–2.2×10^5) were obtained in high yield (>90%), and their stereoregularities were confirmed to be predominantly *cis-transoidal* on the basis of their characteristic laser Raman spectra (Supplementary Figure S1).[24,25] The copolymerization results are summarized in Table 1. The homopolymer of **1L** (poly-**1L**) was also prepared in the same manner for comparison (run 8 in Table 1).[19,20]

We first investigated the effects of the solvent and temperature on chiroptical properties of the copolymers of different ee values and of the homopolymer, as the homopolymer poly-**1L** is very sensitive to the solvent polarity and exhibited a change in the main-chain stiffness (persistent length), accompanied by inversion of the helical sense of the polymer, resulting from the 'on and off' manner of the intramolecular hydrogen bonding networks in polar and nonpolar solvents, respectively, which further results in a change in the cholesteric twist sense.[26] The copolymers poly(**1L**$_m$-*co*-**1D**$_n$) and homopolymer poly-**1L** showed a relatively weak induced CD (ICD) in the π-conjugated polymer backbone regions in a dilute benzene solution at 25 °C (Supplementary Figure S2A), compared with those of analogous helical poly(phenylacetylene)s bearing chiral bulky substituents.[27–33] However, the ICD intensities for poly-**1L** (Supplementary Figure S2B) and poly(**1L**$_m$-*co*-**1D**$_n$) with high ee (>75%) significantly increased with the decreasing temperature accompanied by a large red-shift in the absorption spectra in benzene, whereas poly(**1L**$_m$-*co*-**1D**$_n$) with low ee (<50%) showed almost no temperature-dependent CD intensity change (Figures 2A and C, inset), suggesting that almost no amplification of the helical chirality (negative nonlinear effect), induced by the non-racemic monomer units, took place in benzene.

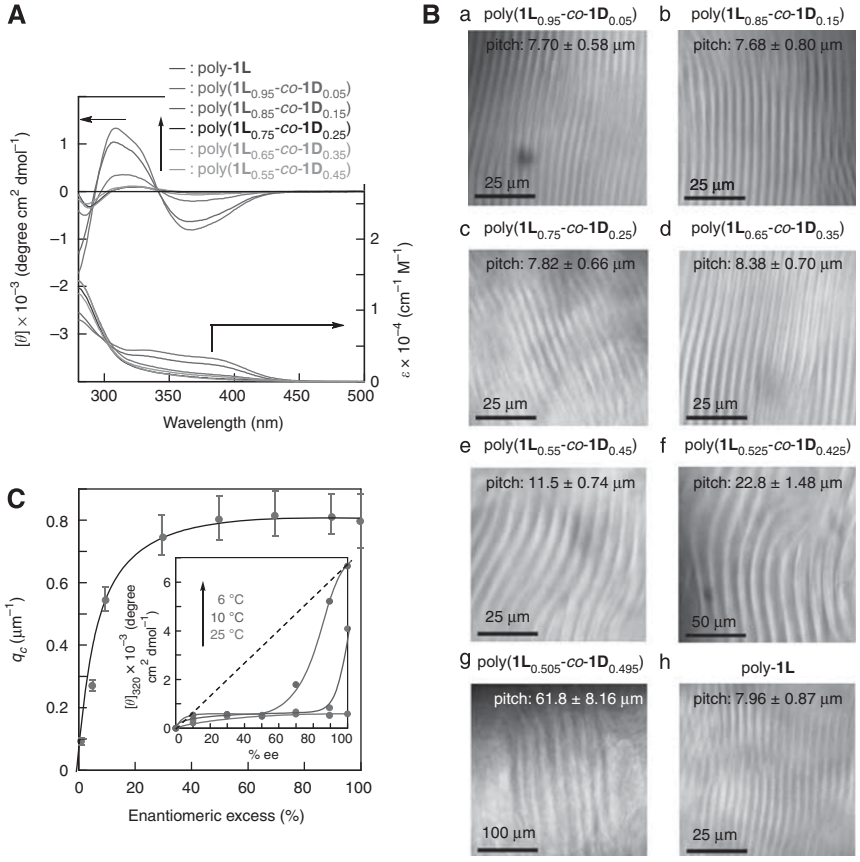

Figure 2 (**A**) Circular dichroism (CD) and absorption spectra of poly(**1L**$_{0.525}$-*co*-**1D**$_{0.475}$) (red lines), poly(**1L**$_{0.55}$-*co*-**1D**$_{0.45}$) (orange lines), poly(**1L**$_{0.65}$-*co*-**1D**$_{0.35}$) (pink lines), poly(**1L**$_{0.75}$-*co*-**1D**$_{0.25}$) (black lines), poly(**1L**$_{0.85}$-*co*-**1D**$_{0.15}$) (green lines), poly(**1L**$_{0.95}$-*co*-**1D**$_{0.05}$) (blue lines) and poly-**1L** (purple lines) in dilute benzene solutions (0.3 mg ml^{-1}) at 6 °C. (**B**) Polarized optical micrographs of cholesteric liquid-crystalline (LC) phases of poly(**1L**$_{0.95}$-*co*-**1D**$_{0.05}$) (a), poly(**1L**$_{0.85}$-*co*-**1D**$_{0.15}$) (b), poly(**1L**$_{0.75}$-*co*-**1D**$_{0.25}$) (c), poly(**1L**$_{0.65}$-*co*-**1D**$_{0.35}$) (d), poly(**1L**$_{0.55}$-*co*-**1D**$_{0.45}$) (e), poly(**1L**$_{0.525}$-*co*-**1D**$_{0.475}$) (f) and poly(**1L**$_{0.505}$-*co*-**1D**$_{0.495}$) (g) in 15 wt% benzene solutions taken at ambient temperature (~25 °C). (**C**) Changes in the cholesteric wave number (q_c) and the CD intensity of poly(**1L**$_m$-*co*-**1D**$_n$) at ~320 nm (inset) versus the percentage enantiomeric excess (ee) of the copolymer components (L-rich) in concentrated solutions at ~25 °C and dilute benzene solutions at 25 (red line), 10 (green line) and 6 °C (blue line) (inset), respectively. The error bars represent the s.d. estimated by an evaluation of ~30 fingerprint spacings. A full color version of this figure is available at *Polymer Journal* online.

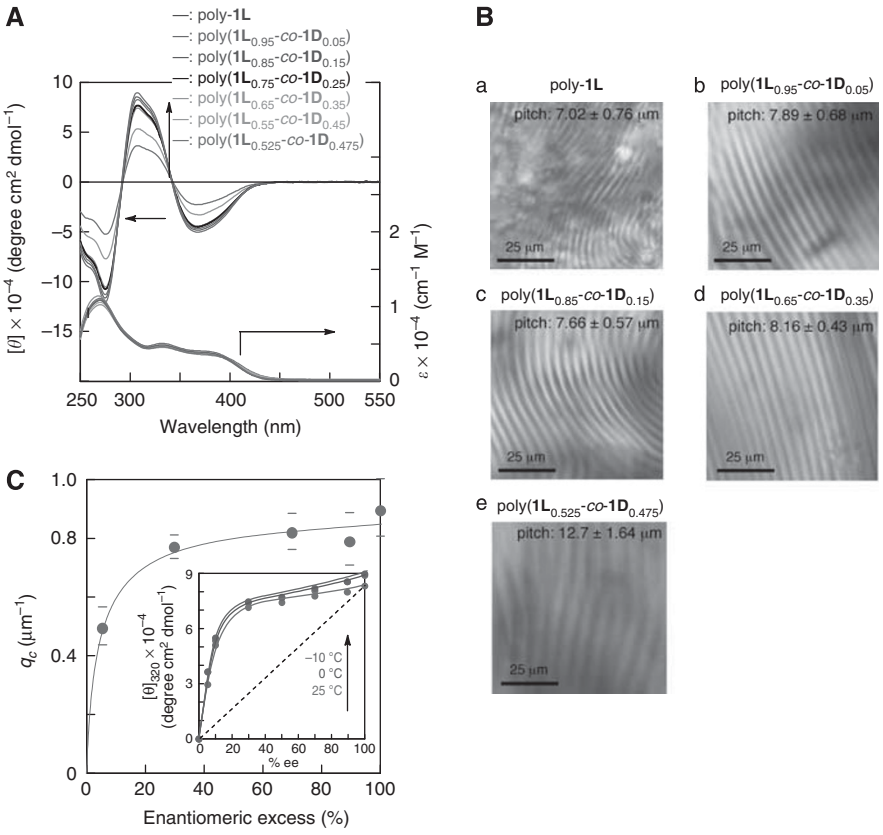

Figure 3 (**A**) Circular dichroism (CD) and absorption spectra of poly(**1L**$_{0.525}$-*co*-**1D**$_{0.475}$) (red lines), poly(**1L**$_{0.55}$-*co*-**1D**$_{0.45}$) (orange lines), poly(**1L**$_{0.65}$-*co*-**1D**$_{0.35}$) (pink lines), poly(**1L**$_{0.75}$-*co*-**1D**$_{0.25}$) (black lines), poly(**1L**$_{0.85}$-*co*-**1D**$_{0.15}$) (green lines), poly(**1L**$_{0.95}$-*co*-**1D**$_{0.05}$) (blue lines) and poly-**1L** (purple lines) in dilute carbon tetrachloride (CCl_4) solutions (0.3 mg ml^{-1}) at 25 °C. (**B**) Polarized optical micrographs of cholesteric liquid-crystalline (LC) phases of poly-**1L** (a), poly(**1L**$_{0.95}$-*co*-**1D**$_{0.05}$) (b), poly(**1L**$_{0.85}$-*co*-**1D**$_{0.15}$) (c), poly(**1L**$_{0.65}$-*co*-**1D**$_{0.35}$) (d) and poly(**1L**$_{0.525}$-*co*-**1D**$_{0.475}$) (e) in 15 wt% CCl_4 solutions taken at ambient temperature (~25 °C). (**C**) Changes in the cholesteric wave number (q_c) and the CD intensity of poly(**1L**$_m$-*co*-**1D**$_n$) at ~320 nm (inset) versus the percentage enantiomeric excess (ee) of the copolymer components (L-rich) in concentrated solutions at ~25 °C and dilute CCl_4 solutions at 25 (red line), 0 (green line) and −10 °C (blue line) (inset), respectively. The error bars represent the s.d. estimated by an evaluation of ~30 fingerprint spacings. A full color version of this figure is available at *Polymer Journal* online.

The reason for these unusual changes in the CD and absorption spectral patterns, and intensities in the longer wavelength regions of the copolymers and homopolymer in benzene is not clear at present; however, a conformational change of the polymer backbones, which may take place in benzene, depending on the ee values of the pendant groups and on temperature, should be taken into consideration.[34,35] Generally, if helical copolymers consisting of non-racemic monomers show a detectable change in their absorption and CD spectra, depending on the ee values of the monomer units, resulting from a conformational change, it is difficult to determine their handedness and to quantify their helix-sense excesses, based on the Cotton effect intensity of the corresponding optically pure homopolymer. In the present study, we assume that the copolymers, poly(**1L**$_m$-*co*-**1D**$_n$), may have a helical conformation different from that of the poly-**IL** in benzene at low temperatures, but with a negligibly small helix-sense excess, thus showing weak ICDs. This hypothesis is supported by the fact that the poly-**1L** maintains its rigid rod-like feature in dilute benzene at 25° C because the persistent length of poly-**1L** estimated in dilute toluene solution, an analogous solvent to benzene, is extremely high (126 nm) at 25° C.[26]

In contrast, the copolymers and homopolymer showed very intense ICDs in nonpolar CCl_4 (Figure 3A), less polar tetrachloroethane (TCE; Figure 4A) and polar THF (Supplementary Figure S3A) even at 25 °C, and their ICD patterns in CCl_4 and benzene at 6 °C are almost mirror images to those in TCE and THF, indicating the inversion of the helicity of the polymer backbones that took place assisted by the solvent polarity, as reported previously for poly-**1L**,[26] poly(**1L**$_m$-*co*-**Aib**$_n$)[19] and other dynamic helical polyacetylenes.[36–44] The CD and absorption spectral patterns in CCl_4, TCE and THF were almost temperature-independent.

Figures 3C and 4C (insets) show the plots of the ICD intensity at ~320 nm of poly(**1L**$_m$-*co*-**1D**$_n$) in CCl_4 and TCE measured at −10 to 25 °C and 25° C, respectively, versus the percentage ee of the components of the copolymers. The ICD intensities increased with the increasing percentage ee of the components and reached an almost constant value at around 30–60 and 30% ee, respectively, thus showing a typical chiral amplification (majority rule), that is, a positive nonlinear effect,[1] whereas the copolymers in THF showed a relatively weak nonlinear relationship (Supplementary Figure S3B). The persistent lengths estimated in dilute CCl_4 and THF at 25° C were 134.5 and 19.2 nm, respectively;[26] this significant decrease of the persistent length in THF may be related to the weak 'majority rule effect'.

We then investigated whether the macromolecular helicity of poly(**1L**$_m$-*co*-**1D**$_n$) in a dilute solution could be further amplified in the lyotropic cholesteric LC state. As previously reported, poly-**1L** and poly-**1D** formed cholesteric LC phases in concentrated solu-

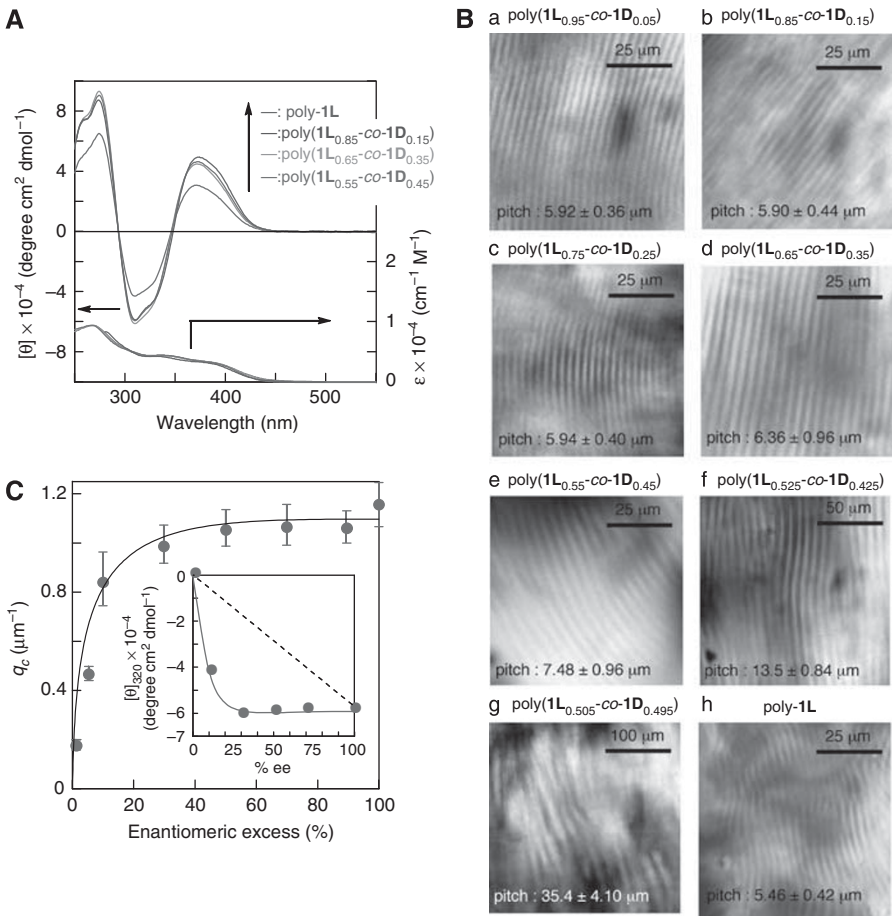

Figure 4 (**A**) Circular dichroism (CD) and absorption spectra of poly(**1L**$_{0.55}$-*co*-**1D**$_{0.45}$) (red lines), poly(**1L**$_{0.65}$-*co*-**1D**$_{0.35}$) (orange lines), poly(**1L**$_{0.85}$-*co*-**1D**$_{0.15}$) (green lines) and poly-**1L** (blue lines) in dilute tetrachloroethane (TCE) solutions (0.3 mg ml^{-1}) at 25 °C. (**B**) Polarized optical micrographs of cholesteric liquid-crystalline (LC) phases of poly(**1L**$_{0.95}$-*co*-**1D**$_{0.05}$) (a), poly(**1L**$_{0.85}$-*co*-**1D**$_{0.15}$) (b), poly(**1L**$_{0.75}$-*co*-**1D**$_{0.25}$) (c), poly(**1L**$_{0.65}$-*co*-**1D**$_{0.35}$) (d), poly(**1L**$_{0.55}$-*co*-**1D**$_{0.45}$) (e), poly(**1L**$_{0.525}$-*co*-**1D**$_{0.475}$) (f), poly(**1L**$_{0.505}$-*co*-**1D**$_{0.495}$) (g) and poly-**1L** (h) in 15 wt% TCE solutions taken at ambient temperature (~25 °C). (**C**) Changes in the cholesteric wave number (q_c) and in the CD intensity of poly(**1L**$_m$-*co*-**1D**$_n$) at ~320 nm (inset) versus the percentage enantiomeric excess (ee) of the copolymer components (L-rich) in concentrated and dilute TCE solutions at 25 °C, respectively. The error bars represent the s.d. estimated by an evaluation of ~30 fingerprint spacings. A full color version of this figure is available at *Polymer Journal* online.

Table 2 Characteristics of poly(1L$_m$-*co*-1D$_n$)

Sample code	q_c[a] (μm^{-1})	% ee_h[b] *(LC)*	% ee_h[c] *(AFM)*	*Helical pitch*[d] *(nm)*	*Chain–chain distance*[d] *(nm)*
poly(**1L**$_{0.505}$-*co*-**1D**$_{0.495}$)	0.10	12	*e*	*e*	*e*
poly(**1L**$_{0.525}$-*co*-**1D**$_{0.475}$)	0.28	34	*e*	*e*	*e*
poly(**1L**$_{0.55}$-*co*-**1D**$_{0.45}$)	0.55	67	89	2.2 ± 0.1	1.9 ± 0.1
poly(**1L**$_{0.65}$-*co*-**1D**$_{0.35}$)	0.75	91	95	2.2 ± 0.1	1.9 ± 0.1
poly(**1L**$_{0.75}$-*co*-**1D**$_{0.25}$)	0.80	98	>99	2.1 ± 0.1	1.9 ± 0.1
poly(**1L**$_{0.85}$-*co*-**1D**$_{0.15}$)	0.82	>99	>99	2.2 ± 0.1	1.9 ± 0.1
poly(**1L**$_{0.95}$-*co*-**1D**$_{0.05}$)	0.82	>99	—	—	—
poly-**1L**	0.80	>99	>99	2.2 ± 0.2[f]	2.0 ± 0.2[f]

Abbreviations: AFM, atomic force microscopy; ee_h, helical-sense excess; LC, liquid crystalline; q_c, cholesteric wave number.
[a]Estimated on the basis of an evaluation of ~30 fingerprint spacings in concentrated solution (15 wt%).
[b]Excess of one helical sense of the copolymers in the liquid-crystalline state, estimated using the maximum q_c=0.82 as the base value.
[c]Excess of one helical sense of the copolymers in the two-dimensional crystals cast from a dilute benzene solution (0.005 mg ml^{-1}) estimated, based on an evaluation of ~1500 helical blocks of poly(**1L**$_m$-*co*-**1D**$_n$) in high-resolution AFM images.
[d]Estimated on the basis of an evaluation of ~100 helical pitches and chain–chain spacings observed in high-resolution AFM images.
[e]Could not be estimated because of difficulty in observing helical structures clearly by AFM.
[f]Data cited from references 44,45.

tions,[19,20,26] and poly(**1L**$_m$-*co*-**1D**$_n$) also formed the cholesteric LC phases in various organic solvents, including benzene, CCl_4 and TCE. Figures 2B, 3B and 4B show the typical optical micrographs of poly(**1L**$_m$-*co*-**1D**$_n$) and poly-**1L** observed in concentrated benzene, CCl_4 and TCE solutions (15 wt%) at ~25 °C, respectively. All copolymers and homopolymer showed a fingerprint texture, typical of the cholesteric LC phases, in which the spacing of the fringes defines half of the cholesteric pitch *p*, and a smaller pitch represents an increased

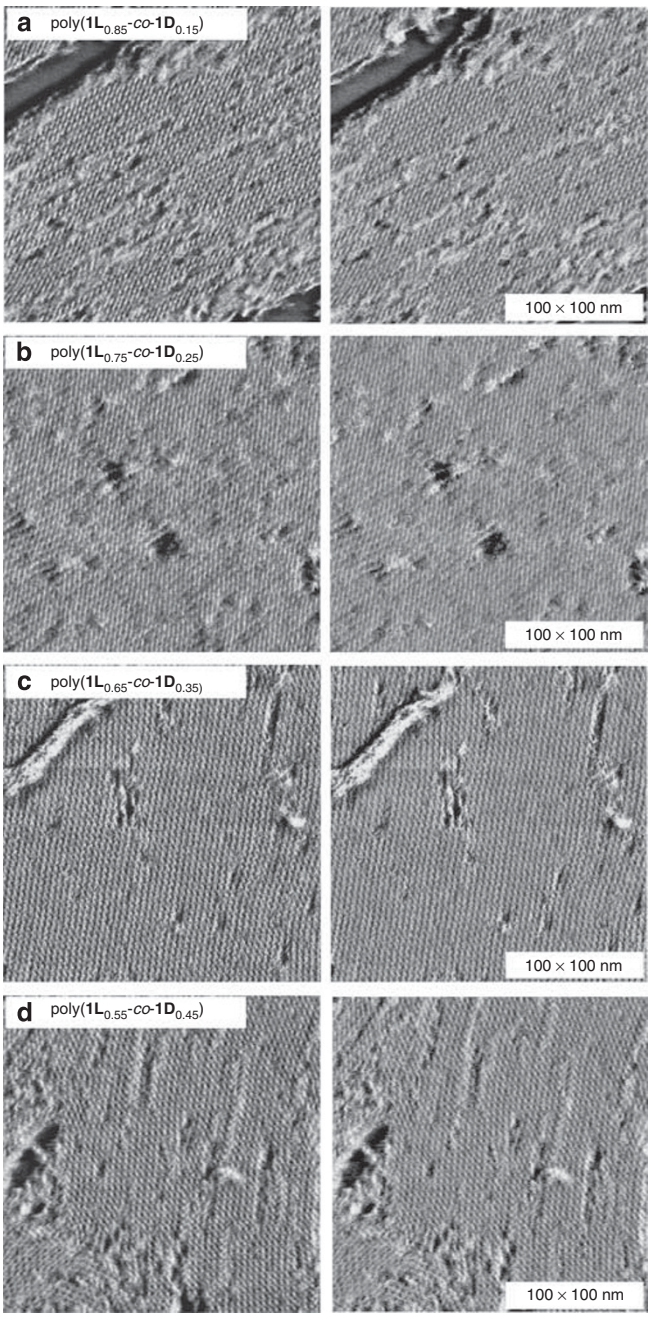

Figure 5 Atomic force microscopy (AFM) phase images of two-dimensional (2D) self-assembled poly(**1L**$_{0.85}$-*co*-**1D**$_{0.15}$) (**a**), poly(**1L**$_{0.75}$-*co*-**1D**$_{0.25}$) (**b**), poly(**1L**$_{0.65}$-*co*-**1D**$_{0.35}$) (**c**) and poly(**1L**$_{0.55}$-*co*-**1D**$_{0.45}$) (**d**) on HOPG. The copolymer strands with clearly identifiable left- and right-handed helical blocks are shown in red and blue colors, respectively (right). Unidentifiable strands are uncolored (black and white). The wide-view AFM phase images are shown in Supplementary Figure S4. A full color version of this figure is available at *Polymer Journal* online.

preference of the one helical sense in the cholesteric phase.[16,45] The plots of the cholesteric wave number q_c, defined by $2\pi/p$ versus the percentage ee of the copolymer components, are shown in Figures 2C, 3C and 4C, respectively. The q_c value of the helical polymer solutions is known to strongly depend on the polymer concentration, temperature and the solvent. If the solution contains enantiomeric or diastereomeric right- and left-handed helices, q_c also depends on the excess of the one helical sense.[15,16,18] Under the constant copolymer concentration of 15 wt% in benzene at ~25 °C, the q_c value of poly(**1L**$_m$-*co*-**1D**$_n$) was found to increase with the increasing percentage ee of the copolymer components, where a larger q_c value means an increased preference of the one-handedness, and the copolymers with 30–50% ee of the components showed as large a q_c value as that of the homopolymer poly-**1L** (100% ee; Figure 2C). This remarkable increase in the q_c value against the percentage ee of the copolymers (positive nonlinear effect) indicated a significant amplification of the helical-sense excess in the LC state, whereas in the dilute benzene solution, chiral information of the pendants that covalently bonded to the copolymer backbone was hardly transformed into a polymer backbone (Figure 2C, inset). Using the maximum q_c value of 0.82 μm^{-1} for the poly-**1L** as the base value, the helical-sense excess (ee_h) of poly(**1L**$_m$-*co*-**1D**$_n$) in concentrated LC benzene solutions can be estimated (Table 2). A similar strong chiral amplification of the macromolecular helicity of poly(**1L**$_m$-*co*-**1D**$_n$) in the LC state was observed in concentrated CCl_4 and TCE solutions (Figures 3C and 4C, respectively). In sharp contrast to the significant amplification of the helical-sense excess of the poly(**1L**$_m$-*co*-**1D**$_n$) in the LC state in benzene over that in the dilute solution, chiral amplification took place at the same level in the LC state and in dilute solutions of CCl_4 and TCE, although the reason for such an unexpected solvent effect observed in benzene on the chiral amplification phenomena in the LC and dilute solutions remains unclear.

The high-resolution AFM images of the self-assembled 2D helix bundle structures of the copolymer chains of poly(**1L**$_m$-*co*-**1D**$_n$) were then measured in order to estimate their ee_h values. Figure 5 shows the typical AFM phase images of poly(**1L**$_m$-*co*-**1D**$_n$) deposited on highly oriented pyrolytic graphite (HOPG) from a dilute benzene solution (0.005 mg ml^{-1}), followed by benzene vapor exposure at ~25 °C for 12 h.[21,22] This method is also very useful for constructing highly ordered 2D helix bundles with a controlled helicity for a dynamically racemic helical poly(phenylacetylene)[23] and helical polyisocyanides[46–48] on HOPG, and their helical structures were visualized by AFM.[49] Poly(**1L**$_m$-*co*-**1D**$_n$) self-assembled into regular 2D helix bundles with a constant height (~1.6 nm), and the copolymer chains packed parallel to each other. These AFM images revealed the helical pitch, helical sense (right- or left-handedness) and molecular arrangements of the copolymers. The periodic oblique stripes observed in each right- or left-handed helical block (blue and red colors in Figure 5 (right), respectively), which originated from a one-handed helical array of the side groups, were tilted clockwise or anticlockwise at +42 and –41°, respectively, with respect to the main-chain axis.[15] Chain-to-chain spacing (~1.9 nm) and helical pitch (~2.2 nm) are similar for the copolymers and homopolymer (Table 2).

Careful observations of the AFM images of the copolymers poly(**1L**$_m$-*co*-**1D**$_n$) (m > n) in Figures 5a–d indicate that the copolymers possess predominantly the left-handed helical array of the pendant groups, which fairly agreed with the previous AFM observation results of the poly-**1L**.[21,22] We note that when poly(**1L**$_m$-*co*-**1D**$_n$) has a left-handed helical array of the pendant groups, the main chain has an opposite, right-handed helical structure.[21,49,50] Although the poly(**1L**$_{0.85}$-*co*-**1D**$_{0.15}$) and poly(**1L**$_{0.75}$-*co*-**1D**$_{0.25}$) consist of a one-handed (left-handed) helical block (Figures 5a and b), the opposite right-handed helical segments were visualized in the AFM images of poly(**1L**$_{0.65}$-*co*-**1D**$_{0.35}$) and poly(**1L**$_{0.55}$-*co*-**1D**$_{0.45}$) (blue colors in Figures 5c and d (right)). On the basis of an evaluation of ~1500 helical blocks, the helical-sense excesses (% ee_h) of poly(**1L**$_{0.85}$-*co*-**1D**$_{0.15}$), poly(**1L**$_{0.75}$-*co*-**1D**$_{0.25}$), poly(**1L**$_{0.65}$-*co*-**1D**$_{0.35}$) and poly(**1L**$_{0.55}$-*co*-**1D**$_{0.45}$) were estimated to be > 99, > 99, 95 and 89%, respectively. When other solvent

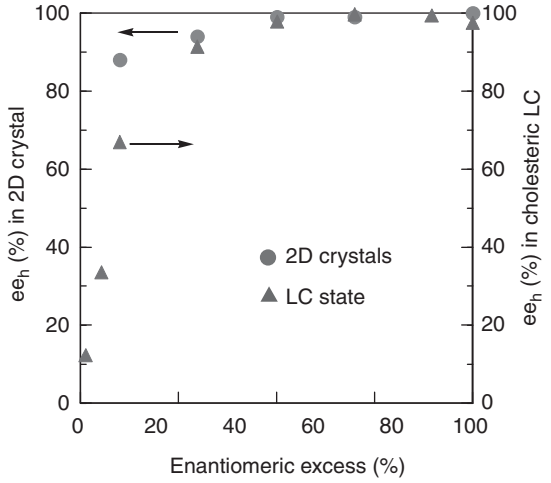

Figure 6 Plots of the helical-sense excess (ee$_h$) values of poly(**1L**$_m$-*co*-**1D**$_n$) versus the percentage enantiomeric excess (ee) of the copolymer components (L-rich) in the cholesteric liquid-crystalline (LC) state in benzene (triangle) and two-dimensional (2D) crystals on HOPG (circle). The ee$_h$ values of poly(**1L**$_m$-*co*-**1D**$_n$) in concentrated LC solutions were calculated using the maximum q_c value of 0.82 as the base value. On the basis of an evaluation of ~1500 helical blocks, the ee$_h$ values of poly(**1L**$_m$-*co*-**1D**$_n$) in the 2D crystals were estimated by atomic force microscopy (Table 2) and Figure 5 and Supplementary Figure S4. A full color version of this figure is available at *Polymer Journal* online.

vapors, such as CCl_4 and TCE, were used, clear 2D helix bundles, suitable for high-resolution AFM observations, could not be formed.

Figure 6 shows the relationships between the ee$_h$ values of poly (**1L**$_m$-*co*-**1D**$_n$), estimated in the cholesteric LC state in benzene and 2D crystals on HOPG, and the percentage ee of the copolymer components. The helical-sense excesses of the copolymers are considerably out of proportion to the percentage ee of the copolymers, demonstrating a greater excess of a single-handed helix via self-assemblies into the lyotropic cholesteric LC state as well as in the 2D crystals. The extent of the departure from linearity in the LC state and in the 2D crystals was almost comparable or slightly greater in the 2D crystals, although we could not precisely determine the ee$_h$ values of poly(**1L**$_{0.525}$-*co*-**1D**$_{0.475}$) and poly(**1L**$_{0.505}$-*co*-**1D**$_{0.495}$) with lower ee (<5%) in the 2D crystals because of difficulty in observing their helical structures clearly by AFM (Table 2). However, the left-handed helical segments appear to be predominant in the copolymer chains on the basis of their high-resolution AFM images. The noticeable chiral amplification observed in the 2D crystals may be attributed to the reduction in the population of the helical reversals between the interconvertible right- and left-handed helical blocks of the poly(**1L**$_m$-*co*-**1D**$_n$) chains, because the kinked helical reversals likely interfere with the close parallel packing of the dynamic helical poly(**1L**$_m$-*co*-**1D**$_n$) chains in the 2D crystals, as proposed for the chiral amplification in the LC state.[15,18,19]

CONCLUSION

In summary, we have observed a unique amplification of the helical-sense excess (majority rule effect) of dynamic helical, LC poly(phenylacetylene)s bearing non-racemic D- and L-alanine residues as the pendant groups in a dilute solution, in the cholesteric LC state and 2D crystal on substrate. The preferred-handed helical-sense and handedness excess of the copolymers in a dilute solution were sensitive to the solvent polarity and temperature, and amplification of the helical-sense excess was significantly affected by the solvents. In contrast to the poly(phenylacetylene) copolymers consisting of optically pure **1L** and achiral **Aib**,[19] chiral amplification took place at almost the same level in the LC state and in the 2D crystals. The fact that the copolymers showed inversion of the helicity in different solvents implies that the copolymers will form similar 2D helix bundles with an opposite helical sense when exposed to specific solvent vapors. The high-resolution AFM technique combined with the 2D crystal formation on substrate, demonstrated in the present study, will enable us to observe such opposite helical structures and also to determine their helical-sense excesses that may be impossible by other spectroscopic methods. These approaches will contribute to understanding the substantial nature of dynamic helical polymers and also provide a unique 2D chiral surface for chiral recognition composed of helical polymers with a switchable helicity.

ACKNOWLEDGEMENTS

This study was supported by grants from the Japan Science and Technology Agency and the Grant-in-Aid for Scientific Research (S) from the Japan Society for the Promotion of Science (JSPS) are gratefully appreciated.

1 Green, M. M., Peterson, N. C., Sato, T., Teramoto, A., Cook, R. & Lifson, S. A helical polymer with a cooperative response to chiral information. *Science* **268,** 1860–1866 (1995).
2 Eelkema, R. & Feringa, B. L. Amplification of chirality in liquid crystals. *Org. Biomol. Chem.* **4,** 3729–3745 (2006).
3 Palmans, A. R. A. & Meijer, E. W. Amplification of chirality in dynamic supramolecular aggregates. *Angew. Chem. Int. Ed.* **46,** 8948–8968 (2007).
4 Aida, T. & Fukushima, T. Soft materials with graphitic nanostructures. *Phil. Trans. R. Soc. A* **365,** 1539–1552 (2007).
5 Kim, H.- J., Lim, Y.- B. & Lee, M. Self-assembly of supramolecular polymers into tunable helical structures. *J. Polym. Sci., Part A: Polym. Chem.* **46,** 1925–1935 (2008).
6 Pijper, D. & Feringa, B. L. Control of dynamic helicity at the macro- and supramolecular level. *Soft Matter* **4,** 1349–1372 (2008).
7 Green, M. M., Reidy, M. P., Johnson, R. J., Darling, G., O'Leary, D. J. & Willson, G. Macromolecular stereochemistry: the out-of-proportion influence of optically active comonomers on the conformational characteristics of polyisocyanates. The sergeants and soldiers experiment. *J. Am. Chem. Soc.* **111,** 6452–6454 (1989).
8 Green, M. M., Garetz, B. A., Munoz, B., Chang, H., Hoke, S. & Cooks, R. G. Majority rules in the copolymerization of mirror-image isomers. *J. Am. Chem. Soc.* **117,** 4181–4182 (1995).
9 Nakano, T. & Okamoto, Y. Synthetic helical polymers: conformation and function. *Chem. Rev.* **101,** 4013–4038 (2001).
10 Fujiki, M., Koe, J. R., Terao, K., Sato, T., Teramoto, A. & Watanabe, J. Optically active polysilanes. Ten years of progress and new polymer twist for nanoscience and nanotechnology. *Polym. J.* **35,** 297–344 (2003).
11 Maeda, K. & Yashima, E. Dynamic helical structures: detection and amplification of chirality. *Top. Curr. Chem.* **265,** 47–88 (2006).
12 Yashima, E. & Maeda, K. Chirality-responsive helical polymers. *Macromolecules* **41,** 3–12 (2008).
13 Yashima, E., Maeda, K. & Furusho, Y. Single- and double-stranded helical polymers: synthesis, structures and functions. *Acc. Chem. Res.* **41,** 1166–1180 (2008).
14 Yashima, E., Maeda, K., Iida, H., Furusho, Y. & Nagai, K. Helical polymers: synthesis, structures and functions. *Chem. Rev.* **109,** 6102–6211 (2009).
15 Green, M. M., Zanella, S., Gu, H., Sato, T., Gottarelli, G., Jha, S. K., Spada, G. P., Schoevaars, A. M., Feringa, B. & Teramoto, A. Mechanism of the transformation of a stiff polymer lyotropic nematic liquid crystal to the cholesteric state by dopant-mediated chiral information transfer. *J. Am. Chem. Soc.* **120,** 9810–9817 (1998).
16 Maeda, K., Takeyama, Y., Sakajiri, K. & Yashima, E. Nonracemic dopant-mediated amplification of macromolecular helicity in a charged polyacetylene leading to a cholesteric liquid crystal in water. *J. Am. Chem. Soc.* **126,** 16284–16285 (2004).
17 Nagai, K., Maeda, K., Takeyama, Y., Sakajiri, K. & Yashima, E. Helicity induction and chiral amplification in a poly(phenylacetylene) bearing *N,N*-diisopropylaminomethyl groups with chiral acids in water. *Macromolecules* **38,** 5444–5451 (2005).
18 Nagai, K., Sakajiri, K., Maeda, K., Okoshi, K., Sato, T. & Yashima, E. Hierarchical amplification of macromolecular helicity in a lyotropic liquid crystalline charged poly(phenylacetylene) by nonracemic dopants in water and its helical structure. *Macromolecules* **39,** 5371–5380 (2006).
19 Ohsawa, S., Sakurai, S.-i., Nagai, K., Banno, M., Maeda, K. & Yashima, E. Hierarchical amplification of macromolecular helicity of dynamic helical poly(phenylacetylene)s composed of chiral and achiral phenylacetylenes in dilute solution, liquid crystal, and two-dimensional crystal. *J. Am. Chem. Soc.* **133,** 108–114 (2011).

20 Okoshi, K., Sakajiri, K., Kumaki, J. & Yashima, E. Well-defined liquid crystalline properties of rigid-rod helical polyacetylenes. *Macromolecules* **38,** 4061–4064 (2005).
21 Sakurai, S.- I., Okoshi, K., Kumaki, J. & Yashima, E. Two-dimensional hierarchical self-assembly of one-handed helical polymers on graphite toward controlling surface chirality. *Angew. Chem. Int. Ed.* **45,** 1245–1248 (2006).
22 Sakurai, S.- I., Okoshi, K., Kumaki, J. & Yashima, E. Two-dimensional surface chirality control by solvent-induced helicity inversion of a helical polyacetylene on graphite. *J. Am. Chem. Soc.* **128,** 5650–5651 (2006).
23 Sakurai, S.-i., Ohsawa, S., Nagai, K., Okoshi, K., Kumaki, J. & Yashima, E. Two-dimensional helix bundles formation of a dynamic helical poly(phenylacetylene) with achiral pendant groups on graphite. *Angew. Chem. Int. Ed.* **46,** 7605–7608 (2007).
24 Shirakawa, H., Ito, T. & Ikeda, S. Raman-scattering and electronic-spectra of poly(-acetylene). *Polym. J.* **4,** 469–472 (1973).
25 Tabata, M., Tanaka, Y., Sadahiro, Y., Sone, T., Yokota, K. & Miura, I. Pressure-induced *cis to trans* isomerization of aromatic polyacetylenes. 2. Poly((*o*-ethoxyphenyl)acetylene) stereoregularly polymerized using a Rh complex catalyst. *Macromolecules* **30,** 5200–5204 (1997).
26 Okoshi, K., Sakurai, S.-i., Ohsawa, S., Kumaki, J. & Yashima, E. Control of main-chain stiffness of a helical poly(phenylacetylene) by switching on and off the intramolecular hydrogen bonding through macromolecular helicity inversion. *Angew. Chem. Int. Ed.* **45,** 8173–8176 (2006).
27 Yashima, E., Huang, S., Matsushima, T. & Okamoto, Y. Synthesis and conformational study of optically active poly(phenylacetylene) derivatives bearing a bulky substituent. *Macromolecules* **28,** 4184–4193 (1995).
28 Nomura, R., Fukushima, Y., Nakako, H. & Masuda, T. Conformational study of helical poly(propiolic esters) in solution. *J. Am. Chem. Soc.* **122,** 8830–8836 (2000).
29 Morino, K., Maeda, K., Okamoto, Y., Yashima, E. & Sato, T. Temperature dependence of helical structures of poly(phenylacetylene) derivatives bearing an optically active substituent. *Chem. Eur. J.* **8,** 5112–5120 (2002).
30 Percec, V., Aqad, E., Peterca, M., Rudick, J. G., Lemon, L., Ronda, J. C., De, B. B., Heiney, P. A. & Meijer, E. W. Steric communication of chiral information observed in dendronized polyacetylenes. *J. Am. Chem. Soc.* **128,** 16365–16372 (2006).
31 Sakai, R., Otsuka, I., Satoh, T., Kakuchi, R., Kaga, H. & Kakuchi, T. Thermoresponsive on-off switching of chiroptical property induced in poly(4′-ethynylbenzo-15-crown-5)/α-amino acid system. *Macromolecules* **39,** 4032–4037 (2009).
32 Jia, H., Teraguchi, M., Aoki, T., Abe, Y., Kaneko, T., Hadano, S., Namikoshi, T. & Marwanta, E. Two modes of asymmetric polymerization of phenylacetylene having a l-valinol residue and two hydroxy groups. *Macromolecules* **42,** 17–19 (2009).
33 Kakuchi, R., Tago, Y., Sakai, R., Satoh, T. & Kakuchi, T. Effect of the pendant structure on anion signaling property of poly(phenylacetylene)s conjugated to α-amino acids through urea groups. *Macromolecules* **42,** 4430–4435 (2009).
34 Nomura, R., Tabei, J. & Masuda, T. Effect of side chain structure on the conformation of poly(*N*-propargylalkylamide). *Macromolecules* **35,** 2955–2961 (2002).
35 Maeda, K., Kamiya, N. & Yashima, E. Poly(phenylacetylene)s bearing a peptide pendant: helical conformational changes of the polymer backbone stimulated by the pendant conformational change. *Chem. Eur. J.* **10,** 4000–4010 (2004).
36 Yashima, E., Maeda, K. & Sato, O. Switching of a macromolecular helicity for visual distinction of molecular recognition events. *J. Am. Chem. Soc.* **123,** 8159–8160 (2001).
37 Nakako, H., Nomura, R. & Masuda, T. Helix inversion of poly(propiolic esters). *Macromolecules* **34,** 1496–1502 (2001).
38 Morino, K., Maeda, K. & Yashima, E. Helix-sense inversion of poly(phenylacetylene) derivatives bearing an optically active substituent induced by external chiral and achiral stimuli. *Macromolecules* **36,** 1480–1486 (2003).
39 Cheuk, K. K. L., Lam, J. W. Y., Chen, J. W., Lai, L. M. & Tang, B. Z. Amino acid-containing polyacetylenes: synthesis, hydrogen bonding, chirality transcription, and chain helicity of amphiphilic poly(phenylacetylene)s carrying L-leucine pendants. *Macromolecules* **36,** 5947–5959 (2003).
40 Lam, J. W. Y. & Tang, B. Z. Functional polyacetylenes. *Acc. Chem. Res.* **38,** 745–754 (2005).
41 Miyagawa, T., Furuko, A., Maeda, K., Katagiri, H., Furusho, Y. & Yashima, E. Dual memory of enantiomeric helices in a polyacetylene induced by a single enantiomer. *J. Am. Chem. Soc.* **127,** 5018–5019 (2005).
42 Maeda, K., Mochizuki, H., Watanabe, M. & Yashima, E. Switching of macromolecular helicity of optically active poly(phenylacetylene)s bearing cyclodextrin pendants induced by various external stimuli. *J. Am. Chem. Soc.* **128,** 7639–7650 (2006).
43 Fukushima, T., Takachi, K. & Tsuchihara, K. Optically active poly(phenylacetylene) film: chirality inversion induced by solvent vapor and heating. *Macromolecules* **41,** 6599–6601 (2008).
44 Kobayashi, S., Itomi, K., Morino, K., Iida, H. & Yashima, E. Polymerization of an optically active phenylacetylene derivative bearing an azide residue by click reaction and with a rhodium catalyst. *Chem. Commun.* **44,** 3019–3021 (2008).
45 Chandrasekaran, S. *Liquid Crystals* Chapter 4, 2nd edn (Cambridge University Press: Cambridge, 1992).
46 Kajitani, T., Okoshi, K., Sakurai, S.-i., Kumaki, J. & Yashima, E. Helix-sense controlled polymerization of a single phenyl isocyanide enantiomer leading to diastereomeric helical polyisocyanides with opposite helix-sense and cholesteric liquid crystals with opposite twist-sense. *J. Am. Chem. Soc.* **128,** 708–709 (2006).
47 Onouchi, H., Okoshi, K., Kajitani, T., Sakurai, S.-i., Nagai, K., Kumaki, J., Onitsuka, K. & Yashima, E. Two- and three-dimensional smectic ordering of single-handed helical polymers. *J. Am. Chem. Soc.* **130,** 229–236 (2008).
48 Wu, Z.- Q., Nagai, K., Banno, M., Okoshi, K., Onitsuka, K. & Yashima, E. Enantiomer-selective and helix-sense-selective living block copolymerization of isocyanide enantiomers initiated by single-handed helical poly(phenyl isocyanide)s. *J. Am. Chem. Soc.* **131,** 6708–6718 (2009).
49 Kumaki, J., Sakurai, S. I. & Yashima, E. Visualization of synthetic helical polymers by high-resolution atomic force microscopy. *Chem. Soc. Rev.* **38,** 737–746 (2009).
50 Yashima, E. Synthesis and structure determination of helical polymers. *Polym. J.* **42,** 3–16 (2010).

Supplementary Information accompanies the paper on Polymer Journal website (http://www.nature.com/pj)